



ELSEVIER

Contents lists available at ScienceDirect

## Journal of the Mechanics and Physics of Solids

journal homepage: [www.elsevier.com/locate/jmps](http://www.elsevier.com/locate/jmps)

# Scaling strength distributions in quasi-brittle materials from micro- to macro-scales: A computational approach to modeling Nature-inspired structural ceramics



Martin Genet <sup>a,b,\*</sup>, Guillaume Couégnat <sup>c</sup>, Antoni P. Tomsia <sup>a</sup>, Robert O. Ritchie <sup>a,d</sup>

<sup>a</sup> Materials Sciences Division, Lawrence Berkeley National Laboratory, California, USA

<sup>b</sup> Surgery Department, University of California at San Francisco, USA

<sup>c</sup> Laboratoire des Composites Thermostructuraux (CNRS – Univ. Bordeaux – Herakles – CEA), Pessac, France

<sup>d</sup> Department of Materials Science and Engineering, University of California at Berkeley, USA

## ARTICLE INFO

### Article history:

Received 11 November 2013

Received in revised form

16 February 2014

Accepted 20 March 2014

Available online 5 April 2014

### Keywords:

Fracture

Microcracking

Ceramics

Finite element analysis

Computational homogenization

## ABSTRACT

This paper presents an approach to predict the strength distribution of quasi-brittle materials across multiple length-scales, with emphasis on Nature-inspired ceramic structures. It permits the computation of the failure probability of any structure under any mechanical load, solely based on considerations of the microstructure and its failure properties by naturally incorporating the statistical and size-dependent aspects of failure. We overcome the intrinsic limitations of single periodic unit-based approaches by computing the successive failures of the material components and associated stress redistributions on arbitrary numbers of periodic units. For large size samples, the microscopic cells are replaced by a homogenized continuum with equivalent stochastic and damaged constitutive behavior. After establishing the predictive capabilities of the method, and illustrating its potential relevance to several engineering problems, we employ it in the study of the shape and scaling of strength distributions across differing length-scales for a particular quasi-brittle system. We find that the strength distributions display a Weibull form for samples of size approaching the periodic unit; however, these distributions become closer to normal with further increase in sample size before finally reverting to a Weibull form for macroscopic sized samples. In terms of scaling, we find that the weakest link scaling applies only to microscopic, and not macroscopic scale, samples. These findings are discussed in relation to failure patterns computed at different size-scales.

© 2014 Elsevier Ltd. All rights reserved.

## 1. Background and significance

Many materials exhibit a quasi-brittle behavior, *i.e.*, their ultimate failure is triggered by a significant number of local events (in contrast to the purely brittle behavior of many ceramics and glasses), yet it is not preceded by highly dissipative processes associated with large inelastic deformations and strain hardening (as with ductile materials like metals). Such behavior is found in geological (*e.g.*, rocks), biological (*e.g.*, bone) and engineering/constructional (*e.g.*, ceramic composites, concrete) materials (Bažant, 1999, 2004). In this paper, we are particularly interested in cellular ceramic structures, which have recently found potential high-impact applications in tissue engineering (Deville *et al.*, 2006) and high-performance composites (Munch *et al.*, 2008).

\* Corresponding author at: Lawrence Berkeley National Laboratory, One Cyclotron Road MS62-0237, Berkeley, CA 94720, USA. Tel.: +1 510 486 6809. E-mail address: [mgenet@lbl.gov](mailto:mgenet@lbl.gov) (M. Genet).

One issue with the engineering use of quasi-brittle materials is associated with the statistical and size-dependence of their failure properties, which can make reliable prediction a difficult challenge. Experimental analyses are often of little help as they cannot reach the target failure probabilities required for certification; for example, a prescribed failure probability of  $10^{-6}$  would require  $10^6$  repeated experiments. Moreover, the standard procedures of fracture mechanics, consisting of studying smaller scale samples and then extrapolating the results to larger, more realistically scaled samples, are limited by the lack of methods which are effectively able to “bridge the length-scales”. Thus, for material design and failure prediction of quasi-brittle materials for engineering applications, experimental studies must be augmented by theoretical tools based on mechanical modeling. However, failure can be a complex phenomenon to model, as it involves both local and global phenomena, *i.e.*, small defects induce localized cracks and stress redistribution at nano- to micro-scales coupled with the fact that the macro-scale size of a structure can statistically dictate the probability of activating the worst-case defects.

Many authors have studied the failure of quasi-brittle materials, from such multiple viewpoints. Our objective here is not to draw an exhaustive portrait of the field, but to note several pertinent studies to better position our own approach. A critical analysis is undoubtedly the Weibull theory which describes the failure of brittle (in-series) systems, based on a specific strength (*i.e.*, Weibull) distribution and a power law for the volumetric scaling (Weibull, 1939, 1951; Hild, 2001), together with that of Daniels who established that the corresponding strength distribution of large in-parallel systems must tend toward a Gaussian distribution (Daniels, 1945). These analyses are essential for the understanding of the statistical failure of quasi-brittle materials. They have been extended by many authors to account for, *e.g.*, multiaxial fracture in Weibull theory (Evans, 1978; Guillaumat and Lamon, 1996), or different load sharing mechanisms in Daniels theory (Phoenix, 1974, 1978; Calard and Lamon, 2004). They are, however, limited in their application to realistic systems, as for example with Daniels theory which fails to describe the transition from Weibull to Gaussian behavior, and to predict the distribution's tail (which cannot be Gaussian) (Bažant, 2004; Bažant and Pang, 2007).

With respect to cellular ceramics, Gibson and Ashby (1997) derived the structure-stiffness relationships for many porous structures simply using beam and plate theories, although their approach cannot directly treat the statistical and size-dependent aspects of failure.

Similar micromechanical approaches have been proposed for many biological and synthetic quasi-brittle materials, *e.g.*, Ji and Gao (2004) and Begley et al. (2012), but again the key stochastic and size-dependent aspects of quasi-brittle failure were not directly considered. (These analyses are invariably based on a single representative volume element, where Cox's, 1952 shear lag principle is used to estimate the redistribution of stresses around cracks.)

There are also the purely macroscopic approaches, *e.g.*, De Borst et al. (1995), Desmorat et al. (2007), and Genet et al. (2013b); but as these analyses are based on continuum damage mechanics (Lemaître and Desmorat, 2005; Lemaître et al., 2009), they cannot explicitly model microstructure or microscopic damage processes, but only their indirect effect on the macroscopic mechanical properties. They are, however, extremely efficient at dealing with specific structures and loads, but require a large amount experimental data for calibration, and are not suitable to derive true structure-properties relationships.

An intermediate approach is that of Bažant et al. (Bažant et al., 1991; Bažant and Xi, 1991; Bažant, 1999, 2004). Based on energetic principles, these authors were able to derive scaling laws for the strength of various quasi-brittle materials, although this method does not permit the scaling of the distributions themselves (Bažant, 2004). More recently, they introduced a hierarchical model of chains and bundles of representative volume elements (RVEs), starting from the atomic scale, to derive some fundamental conclusions on the theoretical scaling of strength in quasi-brittle systems (Bažant and Pang, 2007; Bažant et al., 2009; Le et al., 2011; Le and Bažant, 2011). Most importantly, they were able to predict the transition from Gaussian to Weibull of the strength distributions of structures of increasing sizes (Bažant and Pang, 2007).

In a recent article, we presented our first approach to bridge the scales, with a model based on Sanchez-Palencia's theory of periodic homogenization and Weibull's theory of statistical failure (Genet et al., 2013a), with application to robocast scaffolds (Houmard et al., 2013). Material structure is introduced at microscopic scales, while the sample size is naturally handled on the macroscopic level, the two dimensions being linked through homogenization; statistical failure is then predicted through the computation of a Weibull-like integral at both size-scales. This approach not only has significant predictive capabilities but also has limitations; as the successive failure of the material's constituents is not explicitly represented, a virtual, *ad hoc*, “macroscopic” crack population is introduced, which must be identified experimentally on the macroscopic scale.

In the present paper, we propose a computational method to directly link the strength distributions of the constituents of quasi-brittle materials and macroscopic samples made from these constituents. The idea is to overcome the intrinsic limitations of approaches based on a single RVE, which are really only suitable to deal with homogeneous phenomena (on the scale of the structure), but not strictly with localized events such as those triggering failure. We achieve this by modeling as many RVEs as necessary to produce reliable predictions. Since the number of RVEs that can be modeled at a microscopic level of description is rapidly limited by computational capabilities, we introduce a multi-level numerical method which permits the computation of samples of virtually any size, with essentially no loss of information compared to a direct microscopic computation but with a drastically reduced computational cost. Micro-cells, where physical mechanisms are finely described, are replaced by mechanically and statistically equivalent “macro-cells” containing only a very few degrees of freedom. As a consequence, structural-level computations can be run at a very reduced cost, and a large number of stochastic cases can be explored in a reasonable time.

Fundamentally, we build upon Bažant and Pang (2007), Bažant et al. (2009), Le et al. (2011), and Le and Bažant (2011) and study the scaling of strength induced by both the intrinsic micro-scale defects and the ones generated by the microstructure itself, *i.e.*, the stress redistribution induced by its geometrical features. An important difference with these previous works is that we do not need to idealize the considered microstructure as a series of chains and bundles since we perform direct numerical computations on the real microstructure. Thus, stress redistributions are directly induced by the laws of continuum mechanics and the features of the studied microstructure itself, without any additional assumptions.

Our approach is general, and can be applied to any cellular ceramic, indeed to any quasi-brittle material. We illustrate the methodology here with reference to the ceramic scaffolds that can be made by freeze-casting (Deville et al., 2006; Munch et al., 2008; Naglieri et al., 2013). In order to focus on the method itself, which is presented in Section 2.2, we first develop a simple micromechanical model (Section 2.1), and then present some key results, including numerical validation (Section 3.3), comparison to a basic power law (in-series) scaling (Section 3.2), and application to macro-scale samples (Section 3.4).

## 2. Modeling and methods

### 2.1. The reference micromechanical model

Our approach in this paper is on the failure prediction of porous ceramic scaffolds made by freeze-casting (Deville et al., 2006; Munch et al., 2008; Naglieri et al., 2013). A scanning electron microscopy (SEM) image of a scaffold is shown Fig. 1(a); our associated idealized geometry in Fig. 1(b). This geometry consists of a lamellar ceramic framework linked by periodic bridges to give a brick-like structure, which resembles a coarse nacre-like architecture; in the final bio-inspired materials, the pores in between the “bricks” are infiltrated with a compliant phase, *i.e.*, a polymer or metal, to give a highly damage-tolerant “brick-and-mortar” structure (Munch et al., 2008). To focus on the theoretical strategy itself, we have restricted the analysis to in-plane properties, and chosen a simple geometry, perfectly periodic and deterministic, characterized by only three parameters, namely the distances between brick walls and bridges, respectively,  $d_w$  and  $d_b$ , and the thickness,  $e$ , of these walls and bridges (Fig. 1(b)). An additional parameter must also be introduced to fully define the computed microcells, namely the number,  $r$ , of RVEs that they contain. Note that several authors have proposed methods to generate statistical microstructures from images such as the one in Fig. 1(a) (Jeulin, 2001; Torquato, 2002; Couégnat, 2008), although this has not been undertaken in the present model.

With respect to the phenomenology, the macroscopic failure of these cellular ceramics is induced by the successive failures of individual constitutive walls. Such local failures are triggered by the activation of small defects in tension or shear, or by the wall bending in compression. The failures are highly probabilistic because the distributions of sizes and shapes of defects and walls are very broad. There is other important process that appears in compression, that of the crushing of broken walls, which ultimately results in the ceramic scaffold becoming fully fragmented; for the sake of simplicity we do not consider wall bending/crushing in compression in the current variant of the model. (Such crushing in cellular ceramics usually occurs beyond the scope of application of most models, as the material is then fully fragmented and cannot withstand any other load than compression.)

Thus, initially the micromechanical model will only be developed to consider the defect-activated failure of the ceramic walls, which are assumed to display isotropic elastic-brittle behavior with Young's modulus  $E$  and Poisson's ratio  $\nu$ .

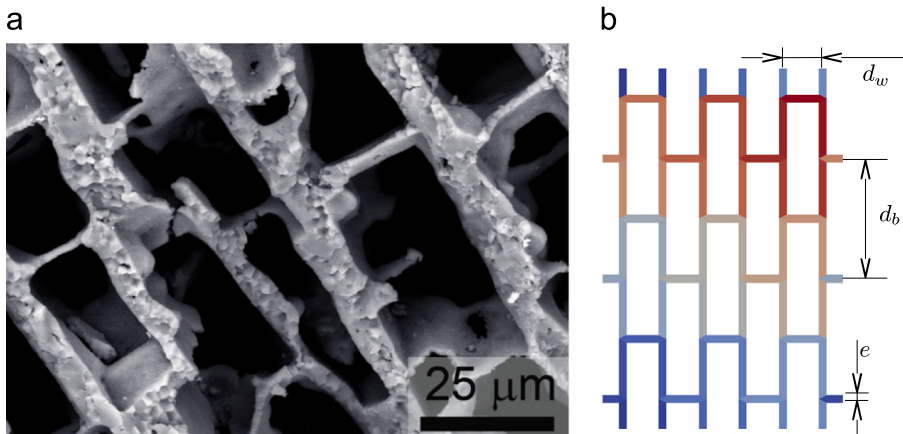


**Fig. 1.** (a) Representative SEM image of a ceramic scaffold made by freeze-casting, and its associated idealized geometry (Launey et al., 2009). (b) The idealized geometry consists of walls connected by bridges positioned in staggered rows. There are three geometrical parameters:  $d_w$  the distance between the walls;  $d_b$  the distance between the bridges;  $e$  the thickness of the walls and bridges. A microcell is defined by  $r \times r$  RVEs. To describe the successive failures of walls and bridges, the scaffold is divided into many elements of volume, represented here in different colors (note the periodicity of the border volume elements). (For interpretation of the references to color in this figure caption, the reader is referred to the web version of this paper.)

**Table 1**

Geometrical coefficients used for the computations presented in this paper:  $d_w$  is the distance between the walls,  $d_b$  the distance between the bridges, and  $e$  the walls and bridges thickness.

$d_w$ ( $\mu\text{m}$ )	$d_b$ ( $\mu\text{m}$ )	$e$ ( $\mu\text{m}$ )
25	75	5

**Table 2**

Material coefficients used for the computations presented in this paper:  $E$  and  $\nu$  are Young's modulus and Poisson's ratio of the walls and bridges;  $V_0$ ,  $\sigma_0$  and  $m$  are the three Weibull coefficients (*i.e.*, reference volume, scale parameter and shape parameter) of the walls and bridges. Note that  $\epsilon_0 = \sigma_0/E$ , in Eq. (1).

$E$ (MPa)	$\nu$ (-)	$V_0$ ( $\text{mm}^2$ )	$\sigma_0$ (MPa)	$m$ (-)
3.5	0.2	1	100	5

The response of the microstructure to mechanical loading is computed using the finite element method. Since the defects are actually too small and too numerous to be characterized, Weibull (1939) theory will be used here to model the wall failures.<sup>1</sup>

As the Weibull theory is a non-local theory of fracture, and we need to represent the successive failures of walls and bridges, they must be split between several elements of volume. This decomposition depends on the considered microstructure, and is illustrated for the freeze-cast scaffold in Fig. 1(b), where every color represents a single element of volume (note the periodicity of the border volume elements). Basically, every bridge is an element of volume, as well as every piece of wall between two bridges. For each element of volume, it is assumed that failure is triggered by positive deformations, a hypothesis often made for brittle and quasi-brittle materials (Mazars and Pijaudier-Cabot, 1989; Lemaître and Desmorat, 2005; Genet et al., 2012; Fagiano et al., 2014), and incorporated in the Weibull framework in Genet et al. (2013a). The failure probability of any given element of volume is then

$$p^F = 1 - \exp\left(-\frac{V}{V_0}\left(\frac{\tilde{\epsilon}}{\epsilon_0}\right)^m\right)$$

$$\text{with } \tilde{\epsilon} = \frac{1}{V} \int_V \|\langle \underline{\epsilon} \rangle_+\| dV \quad (1)$$

where  $V$  is its volume and  $V_0$  is a reference volume,  $\underline{\epsilon}$  is the strain tensor field,  $\langle \cdot \rangle_+$  denotes the positive part of second order symmetric tensors in the classical sense (Lemaître et al., 2009), and  $\epsilon_0$  and  $m$  are, respectively, the two classical Weibull coefficients (Weibull, 1939; Hild, 1998).

Each element of volume contains a potential crack, which is initially closed but will eventually become opened at some point in the computation. Since the position of the crack within the element of volume is not really significant for the remainder of the computation, such cracks will arbitrarily be positioned at the middle of each element of volume.<sup>2</sup> At the beginning of the computation, every element of volume is given a critical probability of failure, *i.e.*, a random number in the range ]0; 1[. During the loading, when the probability of failure of an element of volume reaches its critical value, then it is considered as broken, and the potential crack that it contains is considered open.

This simple model permits the representation of the successive failures of the constituents of a piece of ceramic scaffold of arbitrary size under arbitrary load, from the initial to critical failure event, *i.e.*, from damage initiation to macroscopic crack initiation, and as such provides an assessment of the statistical strength of the scaffold. Note that the model also allows an evaluation of the failure of the walls and bridges at the macroscopic crack tip, *i.e.*, of the propagation of a macroscopic crack, and therefore can provide an assessment of the toughness of the scaffold, although this feature will not be addressed in the present paper.

The geometrical and materials parameters of the freeze-cast ceramic scaffolds used for the computations are presented in Tables 1 and 2.

With respect to the computational procedures, we used GMSH (Geuzaine and Remacle, 2009) (coupled with an in-house Python code) to generate (triangular) meshes, and the LMT++ library (Leclerc, 2010; Genet, 2010) (which uses the CHOLMOD linear solver Chen et al., 2008) for finite element computations.

<sup>1</sup> Despite the fact that it was introduced by Weibull himself based on phenomenological considerations (Weibull, 1939), it was later proven to have more fundamental basis; the theory actually relies upon Poisson's distribution of defect sizes and a simple fracture criterion (Freudenthal, 1968; Hild, 1998; Bažant, 1999). Note that more complex fracture criteria can be used, leading to slightly different laws (Batdorf and Heinisch, 1978).

<sup>2</sup> Note that it was already shown for similar computations that choosing a probabilistic position has no significant effect on the model's predictions (Lamon, 2009).

## 2.2. Computational homogenization-based scaling method for strength distribution

There is actually no theoretical way to scale strength distributions of systems with complex failure patterns such as the one presented in the previous section. In this paper, we propose the computational method to achieve this for any quasi-brittle system illustrated in Fig. 2.

On the macroscopic scale, we have a general continuum mechanics problem, with a sample submitted to boundary conditions and loading (represented here by the external traction  $T$ ). Since the system is probabilistic, its failure will follow a probability law. The objective of our method is to compute this probability law solely based upon the mechanical properties of the sample's constitutive material, without additional assumptions or parameters. To achieve this, the macroscopic problem is discretized and solved using the finite element method, where each element is given a size-dependent and probabilistic mechanical behavior interpolated among a set of responses pre-computed on the microscopic level. It is important to note that the method is not restricted to the study of macroscopically homogeneous systems, but could handle cases, without modification, where, for example, the local material orientation changes from one region to the other, as it is the case for the structure shown in Fig. 1(a).

Pre-computations for a given micro-cell (*i.e.*, geometry of the RVE, number of RVEs, elastic and failure material properties) comprise computing, for a set of macroscopic loading  $\tilde{\Sigma}_i$ , the micro-cell's range of stochastic responses, as illustrated in Fig. 4. A possible set of 2D macroscopic tension load cases is shown in Fig. 3, with canonical (*i.e.*, pure tension in each direction, plus pure shear) and intermediate loading directions. As many sets are possible, it is important to select as many cases as needed for the analysis. The macroscopic finite element behavior is then interpolated between the pre-computed behaviors. In practice, for a given stress  $\underline{\Sigma}$  applied to an element which does not correspond *a priori* to any of the pre-computed cases  $\tilde{\Sigma}_i$ , we compute the associated strain as a linear combination of strains associated with neighboring load cases, using the same interpolation for stresses and strains. One recognizes here the iso-parametric principle used in finite element technology, where the same shape functions are used to interpolate both position and displacement from nodes. Because we are presenting only results on unidirectional load cases, for the computations carried out in this work, we have pre-computed solutions for only one loading direction, which corresponds to the macroscopic loading direction.

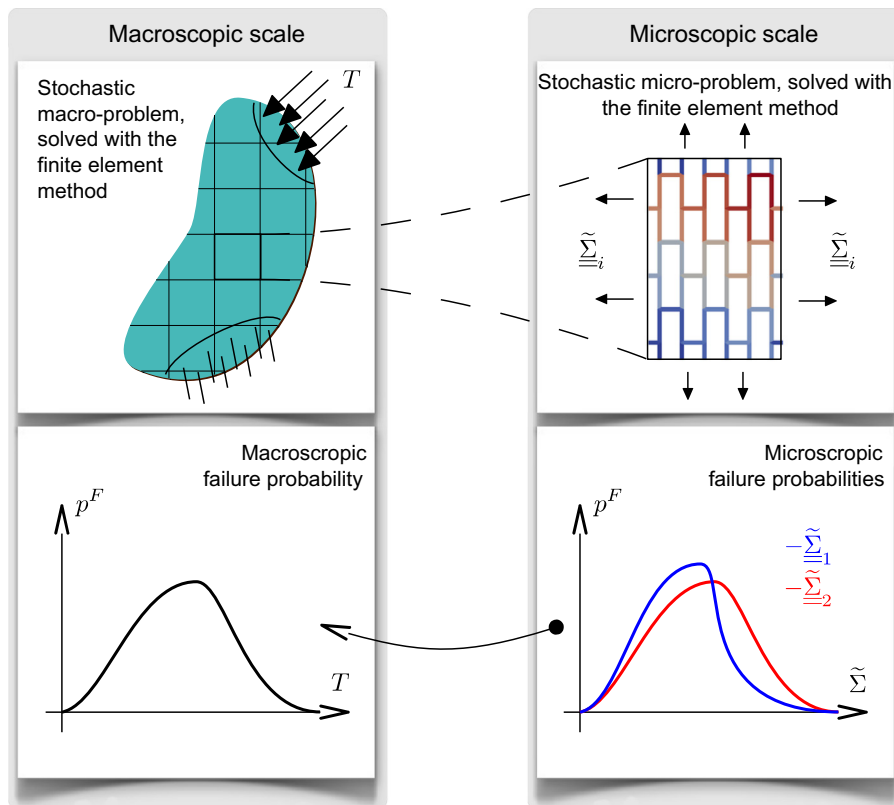


**Fig. 2.** Illustration of our multi-level method. The main goal is to compute the macroscopic failure probability law solely based upon the mechanical properties of the sample's constitutive material on the microscopic level. The macroscopic problem is discretized and solved using the finite element method. Each finite element is given a size-dependent and probabilistic mechanical behavior, interpolated among a set of responses pre-computed on the microscopic level.

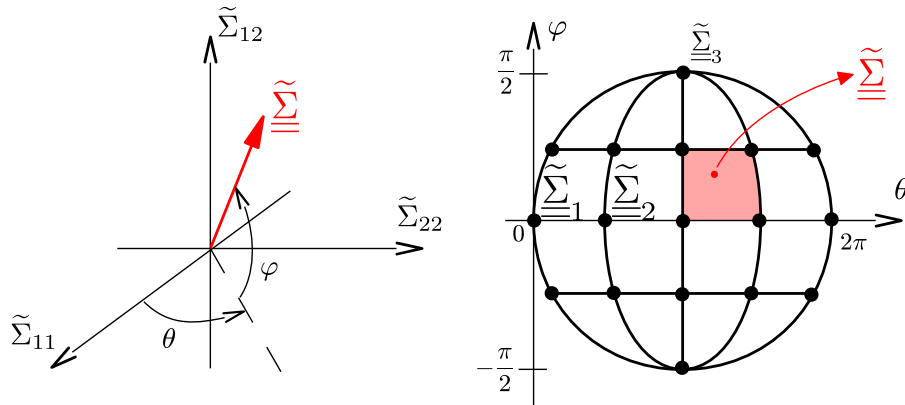


**Fig. 3.** An example of a set of 2D macroscopic loading cases for the stochastic pre-computations on the micro-cell, containing the canonical loading cases  $\tilde{\Sigma}_1$  (pure tension in the bridges direction),  $\tilde{\Sigma}_2$  (pure tension in the wall directions) and  $\tilde{\Sigma}_3$  (pure shear), as well as intermediate cases. For a given macroscopic finite element stress, the behavior is interpolated between the neighboring pre-computed microscopic behaviors.

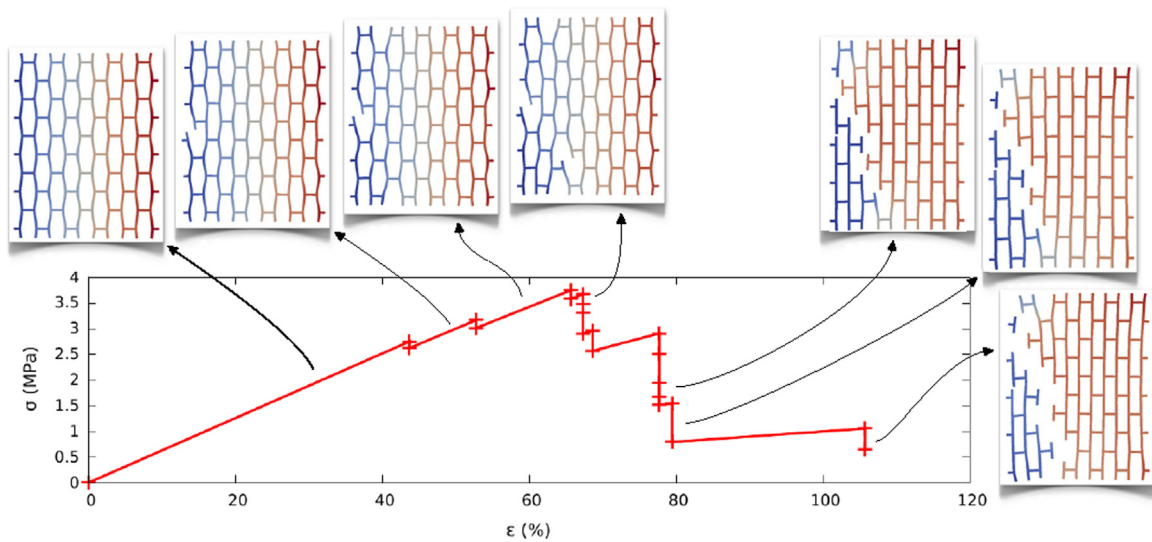


**Fig. 4.** One run of the micromechanical model on a portion of scaffold (size  $r=5 \times 5$  RVEs) under pure traction (plus periodicity conditions), showing the macroscopic stress–strain curve, and displacement fields over the deformed geometries for several reached states. Despite being very basic, the model is able to represent failure of both walls and bridges, eventually outside the main crack, which is not fully orthogonal to the macroscopic loading.

Resulting size effects on the macroscopic level are then directly handled through a competition between microscale failures and multiscale stress redistribution. Our method allows the computation of the strength distribution of any structure under any loading, solely from the stochastic behavior of its constitutive material. Because of this two-level approach, the computation is achieved at a much lower cost than if run directly based upon the micromodel (which would be impossible for macro-scale samples), with virtually no information loss. Let us also point out that if needed, the method could be extended with more than two levels, so that pre-computations would be run scale by scale, from the micromodel up to the desired structural level. Thus, with enough levels of homogenization, the computational cost of solving structural problems becomes low enough to perform thousands, if not millions, of cases in a reasonable time.

On a more technical basis, we implemented the multi-level method using an in-house finite element framework (Couégnat et al., 2013) with the MUMPS library (Amestoy et al., 2000) as a linear solver.

### 3. Results and applications

#### 3.1. Response of the reference micromechanical model

Fig. 4 shows the result of one run of the micromechanical model, previously introduced in Section 2.1, on a portion of scaffold of size  $r=5 \times 5$  RVEs under pure traction with periodic boundary conditions. The resulting stress–strain curve is shown, as well as the strain fields over the deformed geometries for several states reached during the computation. It is

important to note that, even if its ingredients are relatively basic, the present model is already able to capture several fundamental features of actual failures of the ceramic scaffolds, specifically that (i) both bridges and wall failures occur, (ii) bridges and wall failures are present outside the main crack, *i.e.*, there is damage away from the macroscopic crack, (iii) the main crack is not fully straight, and not fully orthogonal to the loading direction.

This micromechanical model can be used to compute the strength distributions of micro-cells of virtually any size, under any loading, with virtually any precision; the actual size of the considered micro-cell is evidently limited by the computational cost, hence the interest of the two-level method presented in this paper. Fig. 5 represents the cumulative strength distribution of micro-cells of size  $r=1 \times 1, 2 \times 2, 4 \times 4, 8 \times 8$  and  $16 \times 16$  RVEs, loaded in tension in the direction parallel to the bridges. Strength distributions are defined as follows: for a given series of  $N$  runs, the strength values are sorted in ascending order, and then assigned a failure probability of  $1/(N+1), 2/(N+1), \dots, N/(N+1)$ . At least 1000 runs were

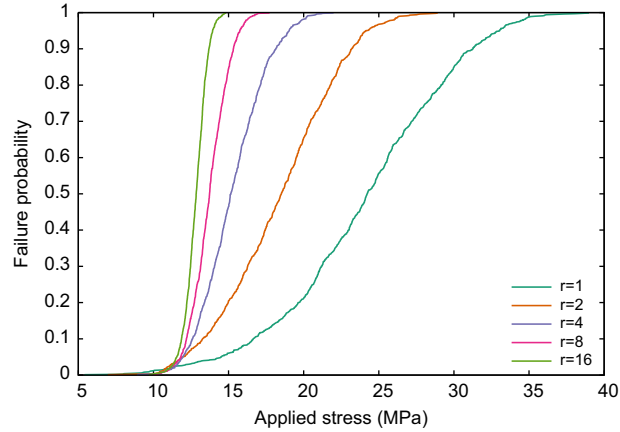


Fig. 5. Strength distribution of successively larger micro-cells (size  $r=1 \times 1, 2 \times 2, 4 \times 4, 8 \times 8$  and  $16 \times 16$  RVEs), highlighting the important size effect in such quasi-brittle structures.

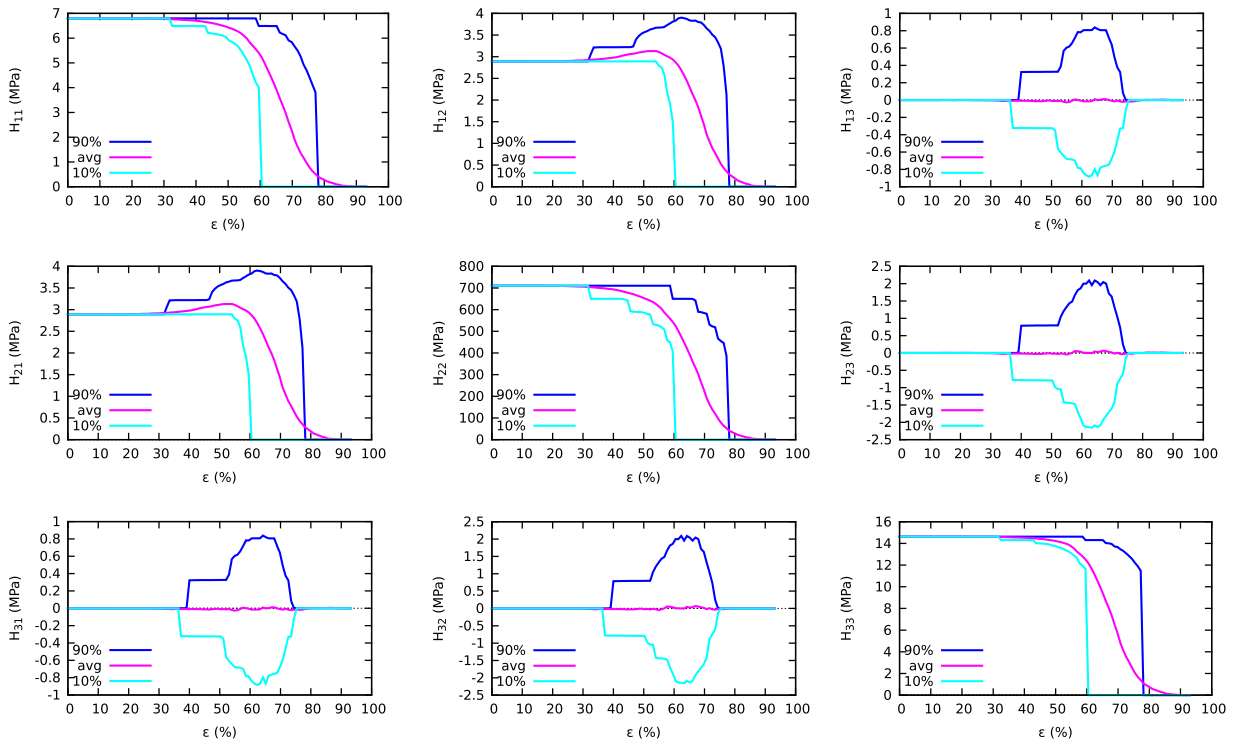


Fig. 6. Distributions of homogenized stiffness tensor components (in matrix notations, Walpole, 1984; François, 1995) ( $H_{ij}$ ) as a function of applied strain ( $\epsilon$ ) on a cell of size  $r=5 \times 5$  RVEs. Cells are loaded in tension in the bridges direction. Mean values, as well as 10% smallest and largest values, are shown to highlight the dispersion. One can see the progressive reduction of mechanical properties associated with successive local failures.

computed for each size, so that the failure probabilities go from  $\approx 0.001$  to  $\approx 0.999$ . This figure clearly illustrates the major size effect in this structure, with an average strength reduced by a factor of two between sizes of  $r=1 \times 1$  and  $r=16 \times 16$ .

In addition to the stress–strain curve and the strength computed on each run, the evolution of the homogenized elastic properties is also calculated for the homogenized computations described in Section 2.2. Thus, for any deformation level, we know the distribution of homogenized stiffness tensors (more precisely, the distributions of their components) of the micro-cells. Fig. 6 shows the distributions, specifically the mean value and those at 10% and 90%, of the components of the homogenized stiffness tensor (using classical matrix notations, Walpole, 1984; François, 1995) as a function of the applied deformation (cells are loaded in tension in the bridges direction) for a cell of size  $r=5 \times 5$  RVEs. It is worth noting that the cell stiffness in both the orthogonal (walls) direction (term  $H_{22}$ ) and the shear (term  $H_{33}$ ) is drastically reduced even if the cell is loaded uniaxially in the bridges direction. This highlights the need to take into account the whole stiffness tensor to accurately simulate the failure process as the stress redistribution between neighboring cells is influenced by their local stiffness.

### 3.2. Limitations of the weakest link theory

Compared to the current method, Weibull's (1939) weakest link theory has many limitations in the scaling of strength distribution in quasi-brittle systems. Basically, it presents a relationship between failure probabilities at different volumes  $V_1$  and  $V_2$  as

$$p^F(V_2) = 1 - (1 - p^F(V_1))^{V_2/V_1} \quad (2)$$

Since this relies on the idea that the failure of a single element of volume induces the failure of the whole structure (more precisely, if  $V_2 > V_1$ , the failure of an element of size  $V_1$  induces the failure of the larger element of size  $V_2$ ), it cannot be strictly applicable for quasi-brittle materials. This is illustrated in Fig. 7, where for several micro-cells of increasing size ( $r=2 \times 2$ ,  $4 \times 4$ ,  $8 \times 8$  and  $16 \times 16$  RVEs), we compare their strength distribution computed using the micromechanical model to the one obtained by scaling the strength distribution of one RVE using Eq. (2). Clearly, the weakest link theory is only valid for the smaller sizes, which are actually brittle and for which the exact and scaled strength distributions match perfectly. This is not the case anymore for the larger sizes, for which several local failures are required to trigger the global failure.

### 3.3. Validation of the computational homogenization-based scaling method for strength distribution

In order to establish the proposed homogenized model, we compared its predictions to those obtained directly with the micromechanical model detailed in Section 2.1. To do so, we created macroscopic meshes equivalent to the microscopic

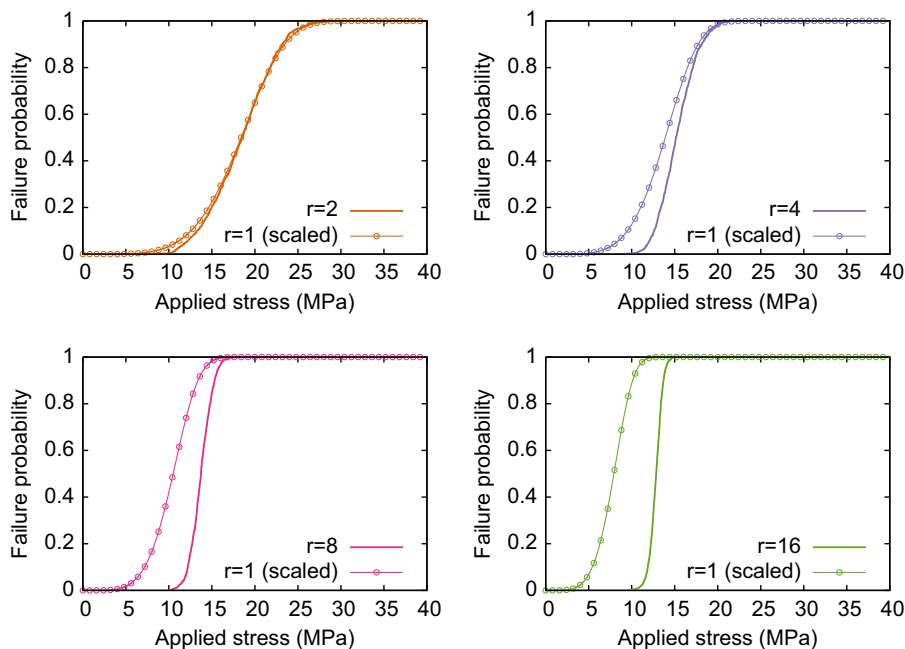
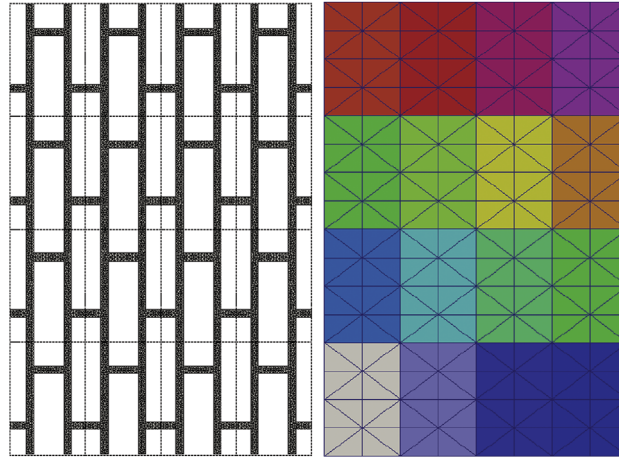
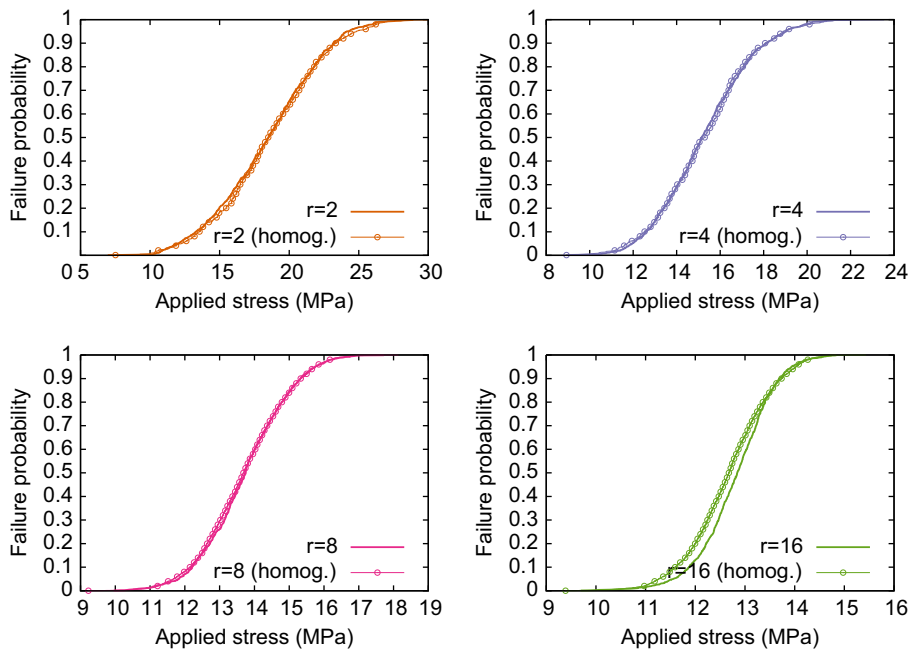


Fig. 7. Comparison between the strength distributions obtained on one RVE and then scaled to a larger volume (circles), and the strength distributions directly obtained on larger micro-cells (solid lines). One can see that the weakest link scaling only applies for very small cells where behavior is brittle.





**Fig. 8.** Finite element mesh of a micro-cell with  $r=4 \times 4$  RVEs (left) and corresponding mesh used for the homogenized computations (right). Each RVE is replaced by a macro-cell of the same size but meshed with only 16 triangular elements.



**Fig. 9.** Comparison of strength distribution predicted by the micro-model (continuous lines) and the homogenized model (circles) for microstructures of various size scales. This establishes the capability of the proposed homogenized model to predict the strength distribution of structures of virtually any size.

ones, where each micro-cell is replaced by a macro-cell of the same shape and size, but meshed with only a few triangular elements, as illustrated in Fig. 8. Note that, in principle, a single quadrangle finite element could have been used for each macro-cell. We have checked that the discretization of the macro-cells did not have any effect on the macroscopic results. The resulting strength distributions are shown in Fig. 9. The predictions based upon the homogenized model match almost perfectly the ones based on the micromechanical model, and this for small sizes (where the final failure is brittle) as well as for larger sizes (where the final failure is induced by many local failures). We also found that the failure patterns were visually similar between the micro- and macro-models. These results prove that it is sufficient to handle the stress redistribution between neighboring RVEs in a homogenized manner. As each RVE exhibits a brittle failure triggered by the first bridge break, it could be chosen as the minimal failure volume in the structure. Therefore, only the average stress state over the RVE has to be considered with respect to the RVE failure. Moreover, the stiffness reduction in the other directions is captured by the evaluation of the residual mechanical properties for each damage state.

### 3.4. Application to failure prediction of macroscopic scale samples

Based on the homogenized model established in this work, we can now scale the strength distributions obtained on a given micro-cell to virtually any size, thereby enabling the study of the shape and scaling properties of the strength distributions across scales. The ceramic brick-like microstructure studied in the present work (Fig. 1(a)) represents a complex system with in-parallel (*i.e.*, where local failures generate over-load on the neighboring constituents) and in-series (*i.e.*, where local failures also unload some neighboring constituents) connections; as such its strength distribution cannot be represented *a priori* by canonical distributions such as the Weibull distribution (as is the case for in-series systems) or a normal distribution (as is the case for large in-parallel systems, Daniels, 1945). Similarly, as evidenced by Fig. 7, except for very small sample sizes the size effect on the strength distributions cannot be described by a simple law such as the power law (as is the case for solely in-series systems). However, it is possible to investigate the shape and scaling properties *a posteriori* from the numerical computations. For instance, Fig. 10 illustrates the evolution of the strength as a function of the size of the considered microstructure, from micro- to macro-scales. One can recognize the size effect that has been documented experimentally for quasi-brittle materials, *e.g.*, Bazant (1999).

Since we compute the entire strength distributions for several sample sizes, it is possible to study their shape and scaling relationships. Fig. 11 shows the fit error (*i.e.*, the distance between the set of points and the fitted law), for both Weibull and normal distribution laws, as a function of the sample size. One can distinguish three domains on the curves: (i) for very small samples, *i.e.*, of the size of RVE, the strength distribution is of Weibull shape, which is consistent with the hypothesis that walls and bridges failure follows a Weibull law and that the brittle failure of the RVE is triggered by the first bridge break; (ii) there is an intermediate domain where strength distribution is closer to a normal distribution than to Weibull; (iii) finally, for macroscopic scale samples, the strength distribution appears to revert to a

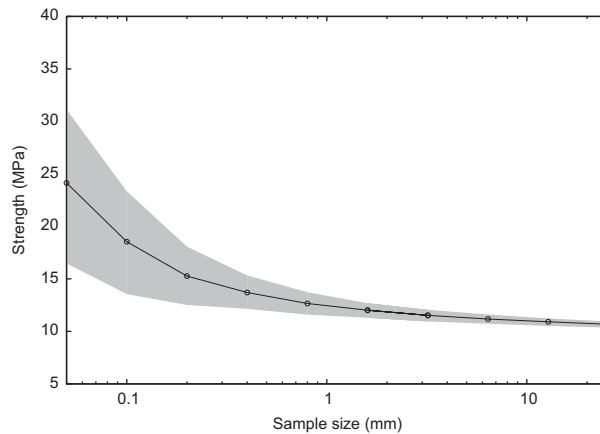


**Fig. 10.** Strength associated with 50% failure probability (continuous line) and range of strength associated with failure probability between 10% and 90% (grey area), as a function of the structure size. The homogenized model based method proposed in this work permits the computation of a very wide range of sizes, from the micro- to the macro-scales. The computed behavior corresponds to what is found experimentally for quasi-brittle materials (Bazant, 1999).

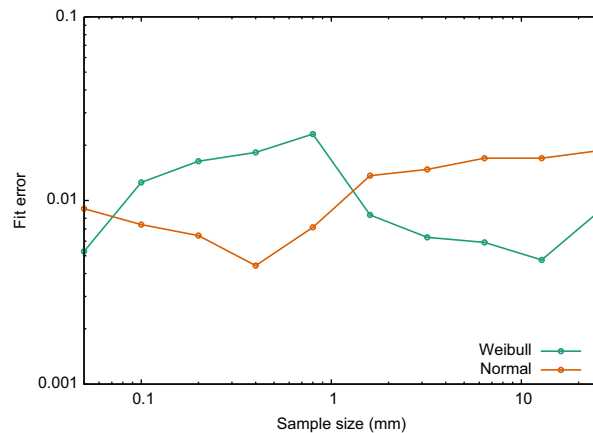


**Fig. 11.** Fit error for both Weibull and normal distribution laws, as a function of the sample size. Strength distributions are of Weibull type for the RVE and macroscopic samples; they are closer to normal type for intermediate sample sizes.

Weibull shape. Note that the parameters of the macroscopic Weibull distribution differ from the ones of the RVE scale and cannot be predicted by simply scaling the RVE scale parameters. The particular relationship between the sets of parameters is indeed an outcome of our method. The conclusions are admittedly linked to the particular system studied in this paper and the hypothesis underlying the chosen micromodel, but our approach does illustrate the prediction capabilities of the proposed method.

Not surprisingly, these findings are similar to the predictions of [Bažant and Pang \(2007\)](#). The only difference is that the initial strength distribution is Weibull-shaped and not Gaussian, which is due to the modeling choices underlying the micromechanical model, especially the fracture model of the material constituents. Here we assumed that the defects triggering failure are at a much lower length scale, so that the constituents failure is well described by a Weibull law, which in turn generates a Weibull-shaped strength distribution for the geometrical RVE.

The above discussion is concerned only with the shape of the strength distribution across scales, but scaling relationships can also be studied. [Fig. 13](#) shows the scaling error (*i.e.*, the distance between the scaled strength distribution and the reference one), supposing a weakest link scaling, as a function of sample size for several cells of increasing size. The strength distribution of cells of size  $r=1 \times 1$  to  $r=64 \times 64$  is scaled up to larger sample sizes using [Eq. \(2\)](#). One can see that for any initial cell size, the scaling error rapidly increases when considering a larger sample. For a cell size of  $r=1$ , the weakest link scaling hypothesis is only relevant for very small samples ( $< 0.1$  mm), as previously discussed in [Section 3.2](#). Even when considering a larger cell size, it is not possible to accurately predict the strength distribution of significantly larger samples. As a consequence, for macroscopic samples, the brittle-like failure of this microstructure is not triggered by the weakest local defects, nor by the failure of a critical volume of material (*i.e.*, by the failure of a cell of size  $r \gg 1 \times 1$ ).

Another way to look at this is to investigate the failure patterns across scales. For very small size samples, failure is fully brittle and is triggered by the first wall or bridge to break. For intermediate size samples, we have seen that the final failure is triggered by the percolation of several bridge/wall breaks, and is mainly governed by the stress redistribution after each break ([Fig. 4](#)). For larger sample sizes, the failure process appears to be different. [Fig. 12](#) illustrates the failure process in a large structure ( $r=256 \times 256$  RVEs). An initial step in the fracture process consists of a widespread development of damage due to the uncorrelated failure of the weakest local defects. Stress redistribution caused by these failures is not significant enough to make the neighboring cells break or to initiate a macrocrack as the clusters of broken cells remain small with a typical size of 2–3 cells. Eventually a critical defect is activated, rapidly leading to the development of an incipient macrocrack which leads to the final failure of the specimen. It is important to distinguish this type of “brittle-like” failure from a failure that would be induced by many correlated events. The “fatal” macrocrack does not result from the percolation of previously damaged cells; moreover, the location of the critical defect is not necessarily within the most damaged area of

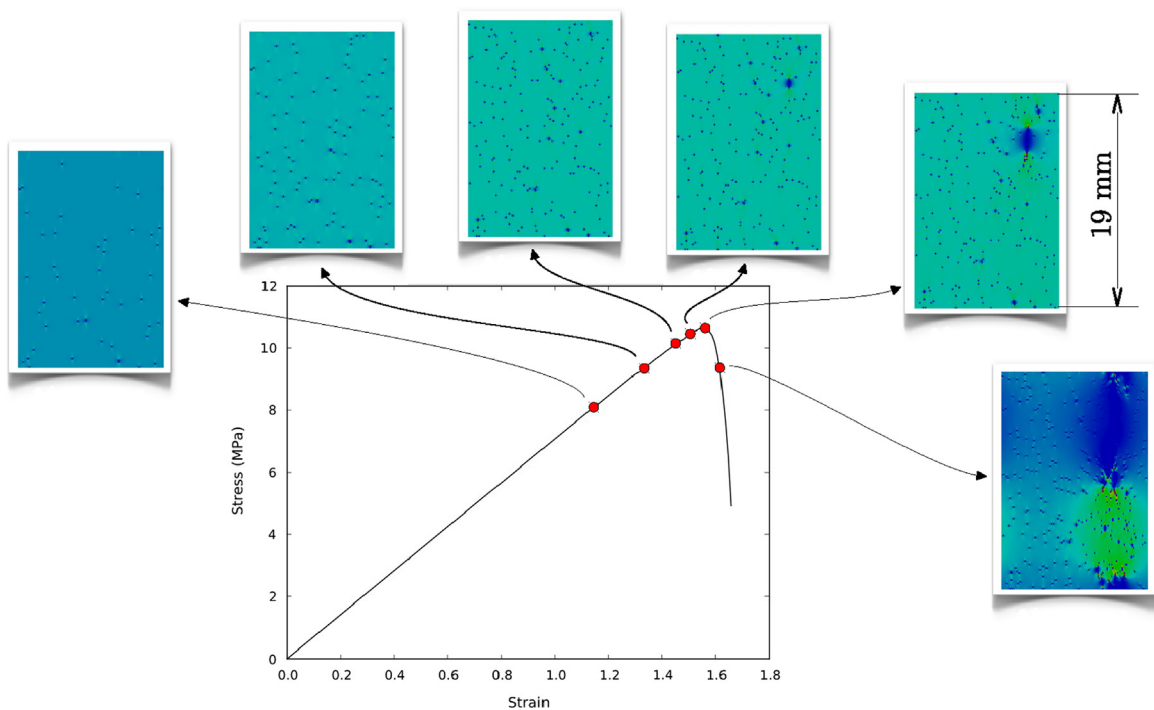


**Fig. 12.** Stress–strain curve and stress field snapshots for one run of the homogenized model on a large scaffold (size  $r=256 \times 256$  RVEs) under traction (plus periodicity conditions), with stress–strain curve and stress fields (dark blue zones correspond to zero level stress, *i.e.*, broken RVEs) over the deformed geometries at multiple time points, showing that macroscopic failure is induced by the sudden activation of a macroscopic defect. (For interpretation of the references to color in this figure caption, the reader is referred to the web version of this paper.)

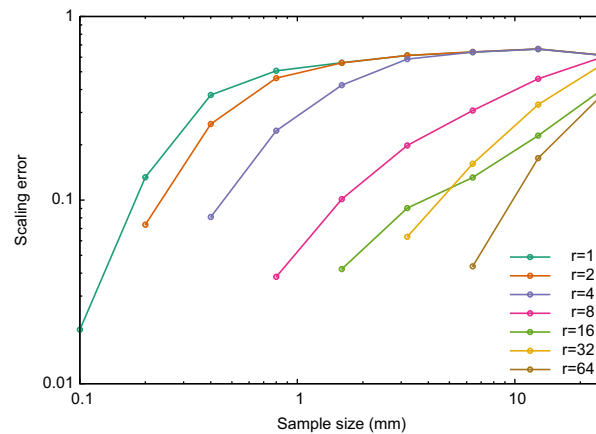


**Fig. 13.** Scaling error for several cells of increasing size  $r \times r$  as a function of the sample size considering a weakest link scaling law, showing that weakest link scaling only applies on the very small samples.

the specimen. It appears that two populations of defects can be identified: (i) a population of non-critical defects corresponding to the weakest local defects activated at a low stress level; and (ii) a population of critical defects, uncorrelated from the first ones, which can lead to the brittle failure of the specimen. Indeed, this represents another example why it is possible to predict the failure of similar materials based on an *ad hoc* description of the critical defects population, as previously shown by the authors (Genet et al., 2013a).

#### 4. Summary and perspectives

We have presented a multi-level numerical method which provides the means to derive reliable structure–strength relationships including statistical and size-dependent aspects, suitable to virtually any quasi-brittle material and any engineering component made from it. There are numerous potential applications with this methodology. Such models can be used by material engineers to optimize fabrication processes to optimize their microstructures in a quantitative way; they can also be used by mechanical or civil engineers to perform reliability analysis and derive optimum designs for specific applications.

The methodology also provides some fundamental insight to the failure of quasi-brittle systems, a subject of widespread interest for many decades, but rarely studied in its full complexity to include statistical and size-dependent effects. With this approach, we were able to determine three domains of failure patterns. Our most important conclusion is that the shape of the strength distribution, after being closer to normal for intermediate scale samples, reverts to Weibull for macroscopic scale samples. The Weibull coefficients of the macroscopic law are different compared to the ones of the microscopic law, and the link between the two sets of parameters is an outcome of the method. This conclusion is in qualitative agreement with Bažant's theory (Bažant and Pang, 2007). An immediate perspective of this work will be to perform quantitative comparisons between our numerical predictions and this theory. However, it is important to point out that once the micromechanical model is defined, our approach does not require any additional assumption to predict the scaling laws. Thus, the number of “chains” and “bundles” of the equivalent hierarchical microstructure required in the Bažant model could be identified directly by our approach.

This capability of our approach allows us to use it to provide guidelines for the processing of optimized Nature-inspired materials. Indeed, as our intent here was to focus on the method itself, we used a simplistic micromechanical model, but we plan now to study the effect of varying microstructural parameters and the introduction of different toughening mechanisms on the scaling laws of a given material. These variations will impact the geometrical RVE failure distribution, as well as the length scales at which transition between Weibull and Gaussian descriptions occur, *i.e.*, the size of the “failure RVE”, which is predicted by our approach.

Another limitation of this work is that we have studied behavior under only one loading direction, in which the chosen structure has mixed in-series and in-parallel volume elements. We plan to study the other directions, where the system is mostly in-parallel. More generally, we plan to perform homogenized computations where the local behavior is interpolated between microscopic stress–strain curves corresponding to different loading directions to explore the effect of multi-axial loading on the stress redistribution and the failure patterns. Additionally, our intent is to examine the outcome of the method when the local behavior is not obtained on a micro-cell of size  $r=1 \times 1$  RVE, as is the case in the present study, but instead on larger micro-cells, or even with the homogenized model itself.

## Acknowledgment

This work was supported by the Mechanical Behavior Materials Program at the Lawrence Berkeley National Laboratory by the Director, Office of Science, Office of Basic Energy Sciences, Division of Materials Sciences and Engineering of the U.S. Department of Energy under Contract no. DE-AC02-05CH11231.

## References

- Amestoy, P.R., Duff, I.S., L'Excellent, J.-Y., 2000. Multifrontal parallel distributed symmetric and unsymmetric solvers. *Comput. Methods Appl. Mech. Eng.* 184 (April (2–4)), 501–520, [http://dx.doi.org/10.1016/S0045-7825\(99\)00242-X](http://dx.doi.org/10.1016/S0045-7825(99)00242-X). ISSN 00457825.
- Batdorf, S.B., Heinisch, H.L., 1978. Weakest link theory reformulated for arbitrary fracture criterion. *J. Am. Ceram. Soc.* 61 (July (7–8)), 355–358, <http://dx.doi.org/10.1111/j.1151-2916.1978.tb09327.x>. ISSN 0002-7820.
- Bazant, Zdeněk P., 1999. Size effect on structural strength: a review. *Arch. Appl. Mech.* 69, 703–725.
- Bazant, Zdeněk P., 2004. Scaling theory for quasibrittle structural failure. *Proc. Natl. Acad. Sci. U.S.A.* 101 (September (37)), 13400–13407, <http://dx.doi.org/10.1073/pnas.0404096101>. ISSN 0027-8424.
- Bazant, Zdeněk P., Pang, Sze-Dai, 2007. Activation energy based extreme value statistics and size effect in brittle and quasibrittle fracture. *J. Mech. Phys. Solids* 55 (January (1)), 91–131, <http://dx.doi.org/10.1016/j.jmps.2006.05.007>. ISSN 00225096. URL (<http://linkinghub.elsevier.com/retrieve/pii/S0022509606001025>).
- Bazant, Zdeněk P., Xi, Yunping, 1991. Statistical size effect in quasi-brittle structures: II. Nonlocal theory. *J. Eng. Mech.* 117 (11), 2609–2622.
- Bazant, Zdeněk P., Xi, Yunping, Reid, Stuart G., 1991. Statistical size effect in quasi-brittle structures: I. Is Weibull theory applicable?. *J. Eng. Mech.* 117 (November (11)), 2609–2622, [http://dx.doi.org/10.1061/\(ASCE\)0733-9399\(1991\)117:11\(2609\)](http://dx.doi.org/10.1061/(ASCE)0733-9399(1991)117:11(2609)). ISSN 0733-9399.
- Bazant, Zdeněk P., Le, Jia-Liang, Bazant, Martin Z., 2009. Scaling of strength and lifetime probability distributions of quasibrittle structures based on atomistic fracture mechanics. *Proc. Natl. Acad. Sci. U.S.A.* 106 (July (28)), 11484–11489, <http://dx.doi.org/10.1073/pnas.0904797106>. ISSN 1091-6490. URL (<http://www.pubmedcentral.nih.gov/articlerender.fcgi?artid=2710678&tool=pmcentrez&rendertype=abstract>).
- Begley, Matthew R., Phillips, Noah R., Compton, Brett G., Wilbrink, David V., Ritchie, Robert O., Utz, Marcel, 2012. Micromechanical models to guide the development of synthetic ‘brick and mortar’ composites. *J. Mech. Phys. Solids* 60 (August (8)), 1545–1560, <http://dx.doi.org/10.1016/j.jmps.2012.03.002>. ISSN 00225096.
- Calard, Vincent, Lamon, Jacques, 2004. Failure of fiber bundles. *Compos. Sci. Technol.* 64 (April (5)), 701–710, <http://dx.doi.org/10.1016/j.compscitech.2003.07.003>. ISSN 02663538. URL ([www.scopus.com](http://www.scopus.com)).
- Chen, Yanqing, Davis, Timothy A., Hager, William W., Rajamanickam, Sivasankaran, 2008. Algorithm 887: CHOLMOD, supernodal sparse Cholesky factorization and update/downdate. *ACM Trans. Math. Softw.* 35 (October (3)), 1–14, <http://dx.doi.org/10.1145/1391989.1391995>. ISSN 00983500.
- Couégnat, Guillaume, 2008. Multiscale Approach of the Mechanical Behavior of Composite Materials with Woven Reinforcements (Ph.D. Thesis). Bordeaux 1 University (in French).
- Couégnat, Guillaume, Ros, W., Haurat, T., Germain, C., Martin, Éric, Vignoles, G., 2013. An integrated virtual material approach for ceramic matrix composites. *Ceram. Eng. Sci. Proc.* 33, 83–91, <http://dx.doi.org/10.1002/9781118217542.ch8>.
- Cox, H.L., 1952. The elasticity and strength of paper and other fibrous materials. *Br. J. Appl. Phys.* 3 (March (3)), 72–79, <http://dx.doi.org/10.1088/0508-3443/3/3/302>. ISSN 0508-3443.
- Daniels, H.E., 1945. The statistical theory of the strength of bundles of threads. I. *Proc. R. Soc. A: Math. Phys. Eng. Sci.* 183 (June (995)), 405–435, <http://dx.doi.org/10.1098/rspa.1945.0011>. ISSN 1364-5021.
- De Borst, René, Pamin, J., Peerlings, R.H.J., Sluys, L.J., 1995. On gradient-enhanced damage and plasticity models for failure in quasi-brittle and frictional materials. *Comput. Mech.* 17 (December (1–2)), 130–141, <http://dx.doi.org/10.1007/BF00356485>. ISSN 0178-7675.
- Desmorat, Rodrigue, Gatuignt, Fabrice, Ragueneau, Frédéric, 2007. Nonlocal anisotropic damage model and related computational aspects for quasi-brittle materials. *Eng. Fract. Mech.* 74 (July (10)), 1539–1560, <http://dx.doi.org/10.1016/j.engfracmech.2006.09.012>. ISSN 00137944.
- Deville, Sylvain, Saiz, Eduardo, Nalla, Ravi K., Tomsia, Antoni P., 2006. Freezing as a path to build complex composites. *Science* 311 (January (5760)), 515–518, <http://dx.doi.org/10.1126/science.1120937>. ISSN 1095-9203.
- Evans, Anthony G., 1978. A general approach for the statistical analysis of multiaxial fracture. *J. Am. Ceram. Soc.* 61 (July (7–8)), 302–308, <http://dx.doi.org/10.1111/j.1151-2916.1978.tb09314.x>. ISSN 0002-7820.
- Fagiano, Christian, Genet, Martin, Baranger, Emmanuel, Ladevèze, Pierre, 2014. Computational geometrical and mechanical modeling of woven ceramic composites at the mesoscale. *Compos. Struct.* 112, 146–156, <http://dx.doi.org/10.1016/j.compstruct.2014.01.045>. ISSN 02638223. URL (<http://linkinghub.elsevier.com/retrieve/pii/S0263822314000646>).
- François, Marc, 1995. Identification des symétries matérielles de matériaux anisotropes (Ph.D. thesis).
- Freudenthal, A.M., 1968. *Statistical approach to brittle fracture*. In: Liebowitz, H. (Ed.), *Fracture*. Academic Press, New York, pp. 591–619.
- Genet, Martin, 2010. *Toward a Virtual Material for Ceramic Composites* (Ph.D. thesis). ENS-Cachan (in French).
- Genet, Martin, Marcin, Lionel, Baranger, Emmanuel, Cluzel, Christophe, Ladevèze, Pierre, Mouret, Anne, 2012. Computational prediction of the lifetime of self-healing CMC structures. *Compos. Part A: Appl. Sci. Manuf.* 43 (February (2)), 294–303, <http://dx.doi.org/10.1016/j.compositesa.2011.11.004>. ISSN 1359835X.
- Genet, Martin, Houmard, Manuel, Eslava, Salvador, Saiz, Eduardo, Tomsia, Antoni P., 2013a. A two-scale Weibull approach to the failure of porous ceramic structures made by robocasting: possibilities and limits. *J. Eur. Ceram. Soc.* 33 (April (4)), 679–688, <http://dx.doi.org/10.1016/j.jeurceramsoc.2012.11.001>. ISSN 0955-2219.
- Genet, Martin, Marcin, Lionel, Ladevèze, P., 2013b. On structural computations until fracture based on an anisotropic and unilateral damage theory. *Int. J. Damage Mech.* September, <http://dx.doi.org/10.1177/1056789513500295>. ISSN 1056-7895. URL (<http://ijd.sagepub.com/cgi/doi/10.1177/1056789513500295>).
- Geuzaine, Christophe, Remacle, Jean-François, 2009. Gmsh: a three-dimensional finite element mesh generator with built-in pre- and post-processing facilities. *Int. J. Numer. Methods Eng.* 79 (September (11)), 1309–1331, <http://dx.doi.org/10.1002/nme.2579>. ISSN 00295981.
- Gibson, Lorna J., Ashby, Michael F., 1997. *Cellular Solids: Structure and Properties*, Cambridge Solid State Science Series, second edition, Cambridge University Press, Cambridge, <http://dx.doi.org/10.2277/0521499119> ISBN 0521499119.
- Guillaumat, Laurent, Lamon, Jacques, 1996. Probabilistic-statistical simulation of the non-linear mechanical behavior of a woven SiC/SiC composite. *Compos. Sci. Technol.* 56, 803–808.
- Hild, François, 1998. *Damage, Failure and Scale Bridging in Heterogeneous Materials*. Habilitation, ENS-Cachan (in French).
- Hild, François, 2001. The Weibull law: a model of wide applicability. In: *Proceedings of the NATO Advanced-Study-Institute on Physical Aspects of Fracture*, vol. 32, pp. 35–46.
- Houmard, Manuel, Fu, Qiang, Genet, Martin, Saiz, Eduardo, Tomsia, Antoni P., 2013. On the structural, mechanical, and biodegradation properties of HA/ $\beta$ -TCP robocast scaffolds. *J. Biomed. Mater. Res. Part B: Appl. Biomater.* 101 (October (7)), 1233–1242, <http://dx.doi.org/10.1002/jbmb.32935>. ISSN 1552-4981.
- Jeulin, D., 2001. Morphological characterization and modeling of random structures. In: *Bornert, M., Bretheau, T., Gilormini, P. (Eds.), Homogenization in Mechanics of Materials 1: Random Elastic Materials and Periodic Media*. Hermès edition, pp. 95–132 (in French).

- Ji, Baohua, Gao, Huajian, 2004. Mechanical properties of nanostructure of biological materials. *J. Mech. Phys. Solids* 52 (September (9)), 1963–1990, <http://dx.doi.org/10.1016/j.jmps.2004.03.006>. ISSN 00225096.
- Lamon, Jacques, 2009. Stochastic approach to multiple cracking in composite systems based on the extreme-values theory. *Compos. Sci. Technol.* 69 (August (10)), 1607–1614, <http://dx.doi.org/10.1016/j.compscitech.2009.03.009>. ISSN 02663538.
- Launey, Maximilien E., Munch, Etienne, Alsem, D.H., Barth, H.B., Saiz, Eduardo, Tomsia, Antoni P., Ritchie, Robert O., 2009. Designing highly toughened hybrid composites through nature-inspired hierarchical complexity. *Acta Mater.* 57 (June (10)), 2919–2932, <http://dx.doi.org/10.1016/j.actamat.2009.03.003>. ISSN 13596454.
- Le, Jia-Liang, Bažant, Zdeněk P., 2011. Unified nano-mechanics based probabilistic theory of quasibrittle and brittle structures: II. Fatigue crack growth, lifetime and scaling. *J. Mech. Phys. Solids* 59 (July (7)), 1322–1337, <http://dx.doi.org/10.1016/j.jmps.2011.03.007>. ISSN 00225096. URL (<http://linkinghub.elsevier.com/retrieve/pii/S0022509611000524>).
- Le, Jia-Liang, Bažant, Zdeněk P., Bazant, Martin Z., 2011. Unified nano-mechanics based probabilistic theory of quasibrittle and brittle structures: I. Strength, static crack growth lifetime and scaling. *J. Mech. Phys. Solids* 59 (July (7)), 1291–1321, <http://dx.doi.org/10.1016/j.jmps.2011.03.002>. ISSN 00225096. URL (<http://linkinghub.elsevier.com/retrieve/pii/S0022509611000470>).
- Leclerc, Hugo, 2010. Towards a no compromise approach between modularity, versatility and execution speed for computational mechanics on CPUs and GPUs. In: Allix, Olivier, Wriggers, Peter (Eds.), IV European Conference on Computational Mechanics (ECCM2010), Paris, France.
- Lemaître, Jean, Desmorat, Rodrigue, 2005. *Engineering Damage Mechanics: Ductile, Creep, Fatigue and Brittle Failures*. Springer, Berlin Heidelberg, New York.
- Lemaître, Jean, Chaboche, Jean-Louis, Desmorat, Rodrigue, Benallal, Ahmed, 2009. *Solid Materials Mechanics*, third edition. Dunod, Paris (in French).
- Mazars, Jacky, Pijaudier-Cabot, Gilles, 1989. Continuum damage theory—application to concrete. *J. Eng. Mech.* 115 (2), 345–365.
- Munch, Etienne, Launey, Maximilien E., Alsem, D.H., Saiz, Eduardo, Tomsia, Antoni P., Ritchie, Robert O., 2008. Tough bio-inspired hybrid materials. *Science* 322 (December (59)), 1516–1520, <http://dx.doi.org/10.1126/science.1164865>. ISSN 1095-9203.
- Naglieri, Valentina, Bale, Hrishikesh A., Gludovatz, Bernd, Tomsia, Antoni P., Ritchie, Robert O., 2013. On the development of ice-templated silicon carbide scaffolds for nature-inspired structural materials. *Acta Mater.* 61 (October (18)), 6948–6957, <http://dx.doi.org/10.1016/j.actamat.2013.08.006>. ISSN 13596454.
- Phoenix, S. Leigh, 1974. Probabilistic strength analysis of fibre bundle structures. *Fibre Sci. Technol.* 7, 15–31. URL (<http://www.sciencedirect.com/science/article/pii/0015056874900037>).
- Phoenix, S. Leigh, 1978. Stochastic strength and fatigue of fiber bundles. *Int. J. Fract.* 14, 327–344. URL (<http://link.springer.com/article/10.1007/BF00034692>).
- Torquato, S., 2002. *Random Heterogeneous Materials: Microstructure and Macroscopic Properties*, Springer-Verlag, New York, edition.
- Walpole, L.J., 1984. *Fourth-Rank Tensors of the Thirty-Two Crystal Classes: Multiplication Tables*. ISSN 1364-5021.
- Weibull, Wallodi, 1939. A statistical theory of the strength of materials. *R. Swed. Inst. Eng. Res.* 151.
- Weibull, Wallodi, 1951. A statistical distribution function of wide applicability. *J. Appl. Mech.* September, 293–297.